

Mechanical Properties and Soiling Resistance of Paper with Polyurethane Coating Reinforced with Cellulose Nanomaterials

Sooim Goo,^a Simyub Yook,^a Shin Young Park,^a Wanhee Im,^a and Hye Jung Youn^{a,b,*}

Recently, enhancing the performance of polyurethane (PU) coatings with cellulose nanomaterials (CNM) has been actively researched. Cellulose nanomaterials exhibit considerable potential to increase the mechanical strength of PU coatings due to their high aspect ratios and elastic moduli. In this study, PU reinforced with CNM was coated onto paper to enhance the paper's mechanical strength and soiling resistance. To investigate the reinforcing effect, two different CNM, cellulose nanocrystals (CNC) and 2,2,6,6-tetramethylpiperidine-1-oxyl radical (TEMPO)-oxidized cellulose nanofibers (TOCN), were selected, and suspensions with different ratios of PU and CNM were prepared. After coating the paper with each of them, the mechanical properties of the paper, including tensile strength, folding endurance, and soiling resistance, were evaluated. The mechanical strength and anti-soiling performance of the PU-CNM coated papers were greatly enhanced. Especially, PU-TOCN had superior properties as a durable paper coating despite a low TOCN concentration, less than 2%, because the TOCN crosslinked with PU *via* polyaziridine. Furthermore, the PU-CNM coating protected the paper from being contaminated, which was confirmed by scanning electron microscopy and energy dispersive X-ray mapping. Consequently, durable paper exhibiting soiling resistance was fabricated by coating the paper with PU-TOCN suspensions.

Keywords: Cellulose nanomaterials; Durable paper; Mechanical strength; Polyurethane coating; Soiling resistance

Contact information: a: Department of Forest Sciences, Seoul National University, 1 Gwanak-ro, Gwanak-gu, Seoul 08826, South Korea; b: Research Institute of Agriculture and Life Sciences, Seoul National University, 1 Gwanak-ro, Gwanak-gu, Seoul 08826, South Korea;

* Corresponding author: page94@snu.ac.kr

INTRODUCTION

Polyurethanes (PU) have been used in various applications, such as adhesives, coatings, printing, and medicine, because they have versatile properties owing to the ratio of their hard and soft segments (Osman *et al.* 2003; Chattopadhyay and Raju 2007; Rahimi and Mashak 2013; Hung *et al.* 2014; Cataldi *et al.* 2017). Coatings are an important application because PU exhibit excellent mechanical strength and toughness; good chemical, abrasion, and corrosion resistance; and low-temperature flexibility (Akindoyo *et al.* 2016). Furthermore, PU coating has been used to ensure that fibrous materials are waterproof (Meng *et al.* 2009; Cataldi *et al.* 2019; Mazzon *et al.* 2019).

Recently, waterborne polyurethane (WPU) dispersions, which have low volatile organic compound emissions, have received attention as a type of PU coating, because awareness for the necessity of environmental protection is greater than ever (Fan *et al.* 2015; Zhou *et al.* 2015). Additionally, WPU exhibits desirable physical and chemical

properties, such as low viscosity, which is helpful in the coating processes (Noble 1997). However, the performance of WPU coatings must be enhanced to obtain a similar mechanical strength to solvent-borne PU coatings (Cheng *et al.* 2016). UV-curable WPU coating is a method designed to improve the performance of the WPU coating. The WPU coatings cured under UV irradiation exhibit considerable mechanical strength, chemical resistance, and non-toxicity (Çanak and Serhatlı 2013; Noreen *et al.* 2016), even though they are less resistant to solvent and heat (Chuang *et al.* 2008). Hyper-branched polyurethane (HBPU) that contains a number of functional groups improved the thermal and physical performances of the coating because of its high crosslinking density (Florian *et al.* 2010). Several researchers have ensured the desirable properties of HPBU coating by controlling the ratio of isocyanate groups to hydroxyl groups (Petrović *et al.* 2002; Mishra *et al.* 2012). Recently, research has been active in reinforcing WPU with nano-sized fillers such as silica, ZnO, TiO₂, Fe₂O₃, clay, and cellulose nanomaterials. These nanomaterials can affect not only the mechanical but also the rheological, anti-corrosion, and barrier properties (Rahman *et al.* 2008; Saha *et al.* 2011; Rashvand and Ranjbar 2013; Noreen *et al.* 2016).

Among several nanomaterials, cellulose nanomaterials (CNM), including cellulose nanocrystals (CNC) and cellulose nanofibrils (CNF), are expected to have great potential as fillers due to their morphology, mechanical strength, non-toxicity, biodegradability, and good miscibility with hydrophilic polymer matrices (Abdul Khalil *et al.* 2012; Lei *et al.* 2019). Each CNM exhibits unique properties in terms of charge density and morphology such as the average width and aspect ratio. When compared with CNC, CNF has a higher aspect ratio, *i.e.*, a higher ratio of length to width. With respect to the composite of PU and CNM, it has been reported that CNC with low loading levels showed good dispersion in a WPU matrix and significantly enhanced mechanical strength (Gao *et al.* 2012; Zhang *et al.* 2012). Another study showed that CNC enhanced the stiffness and thermal stability of the nanocomposites by interacting with both the soft and the hard segments of PU to form hydrogen bonds (Rueda *et al.* 2013). Furthermore, 2,2,6,6-tetramethylpiperidine-1-oxyl radical (TEMPO)-oxidized cellulose nanofibers (TOCN) have been investigated to improve the performance of PU-CNM composites. Compared with CNF, TOCN have a high negative charge density and high aspect ratio, which are critical for enhancing the mechanical properties of the PU coating (Cheng *et al.* 2016).

PU coating can be applied in the preparation of paper products that require resistance to abrasion and contamination. In addition, PU enhances the mechanical properties of paper including tensile strength and folding endurance (Guo *et al.* 2014). Some paper grades such as banknotes especially need superior physical properties and durability. These papers should not only have high mechanical strength but also be resistant to contaminants. Little research has been done on PU reinforced with CNM. Most studies on PU coatings have focused on abrasion resistance only (Zhang *et al.* 2012; Wang *et al.* 2015; Fan *et al.* 2016), and no attention has been devoted to soiling resistance (*i.e.*, anti-contamination). In this study, PU was reinforced with CNM and used as a coating on paper. The effects of the CNM on the PU coating in terms of soiling resistance and mechanical strength were studied. To research how different types of CNM affect the reinforcing performance, CNC and TOCN were selected as CNM. Additionally, the soiling mechanism of the coated paper was studied to investigate how the PU-CNM coating protected the paper from contamination.

EXPERIMENTAL

Materials

A PU suspension (35 wt%) was supplied from T&L Co., Ltd. (Yongin, Korea). Polyurethane was synthesized with polycarbonate diols. Polyaziridine, as a crosslinking agent, was purchased from Stahl (Waalwijk, Netherlands). Two types of CNM, CNC, and TOCN, were used. Figure 1 shows the transmission electron microscope (TEM, Carl Zeiss, LIBRA 120, Oberkochen, Germany) image of the CNC and the scanning electron microscope (SEM, Carl Zeiss, Germany) image of the TOCN. CNC was purchased from CelluForce (Montreal, Canada) as a powder; the solid content was 94.5 wt%. The average width and length of the CNC were 6.3 nm and 73.9 nm (the standard deviations were 1.9 nm and 25.6 nm), respectively. The zeta potential of the CNC was -58.5 mV. The CNC were dispersed in deionized water to a concentration of 2 wt% before use. The TOCN was provided by Hansol (Seoul, Korea); the fibril width was $14 \text{ nm} \pm 4 \text{ nm}$. The solid content and zeta potential of the TOCN suspension were 0.95% and -56 mV, respectively. The average width and length of CNM were evaluated by measuring the length and width of several hundred nanofibers from the TEM or SEM images. The zeta potentials of the CNC and TOCN (0.1 wt% suspension) were measured using a Zetasizer (Nano Zs, Malvern Instruments, Ltd. UK) at 25°C. The base paper was made of cotton linter, supplied by KOMSCO (Daejeon, Korea). The properties of the base paper are presented in Table 1.

Table 1. Properties of the Base Paper

Basis Weight (g/m ²)	Thickness (μm)	Tensile Strength (kN/m)	MIT Folding Endurance
90.5 ± 1.6	109 ± 2	9.55	2380 double folds

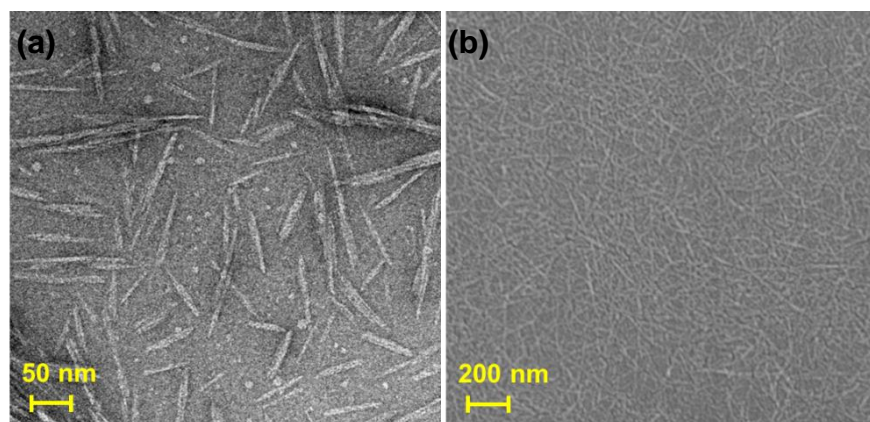


Fig. 1. The (a) TEM image of CNC and (b) SEM image of TOCN

Preparation of PU-CNM Suspensions

The PU suspension was mixed with the CNC and TOCN based on wet weight ratios. The ratio of the mixtures (PU:CNM) was varied as 100:0, 80:20, and 60:40. The mixed PU-CNM suspension was stirred at 600 rpm for 30 min. Polyaziridine was diluted to 50% and then added to the PU-CNM suspension at 4 wt%. The PU-CNM suspension

with polyaziridine was stirred at 600 rpm for 1 h. The suspension was deaerated under vacuum before it was applied as a coating.

Table 2. Mixing Ratios of PU and CNM

CNM Type	CNC		TOCN	
	PU8C2	PU6C4	PU8T2	PU6T4
Mixed Suspension ID	PU8C2	PU6C4	PU8T2	PU6T4
Mixing Ratio (wet base)	80:20	60:40	80:20	60:40
Dry Weight Ratio of CNM Based on PU (%)	1.43	3.81	0.68	1.81
Total Solid Content (%)	28.4	21.8	28.2	21.4

Coating the PU-CNM Suspension on the Paper

The PU-CNM suspensions were coated on the base paper using a laboratory bar coater (Automatic Film Applicator, TQC Sheen, Capelle aan den IJssel, Netherlands). The coating speed was 70 mm/s, and the wire thickness was 4 μm . The coated paper was dried in a hot-air dryer at 120 °C for 2.5 min, after which it was passed through a drum dryer at 100 °C for curing. The coating on the back side of the paper was prepared the same way. The coated papers were conditioned at 23 °C \pm 1 °C and 50% \pm 2% relative humidity for 1 day.

Characterization

Properties of the suspension

To evaluate the dispersion stability of the mixed PU-CNM suspension, the change in light transmittance along the height of a vial was measured for 12 h using a Turbiscan LAB stability analyzer (Formulation, Toulouse, France). Low-shear viscosity was measured by a Brookfield DV2TLV viscometer (Brookfield Engineering Laboratories, Inc., Middleboro, MA, USA) using the no. 4 spindle at 100 rpm for 30 s.

Mechanical strength

The tensile strength of the coated paper was measured in the machine direction according to ISO 1924-2:2 (2008). The folding endurance was measured in the cross-machine direction with ISO 5626 (1993) (MIT test for folding endurance), because banknotes require high folding endurance in the cross-machine direction.

Soiling resistance

Wet and dry soiling resistance tests were conducted. To evaluate the soiling resistance under the wet condition, the coated paper samples were exposed to contaminants composed of ceramic beads, colored powder, artificial sweat, and lanolin. The specimens were fixed with a wooden holder and shaken with the contaminants in a bottle for 10 min, 15 min, and 20 min. The color difference (ΔE) after soiling, compared with that before soiling, was measured to determine the anti-soiling performance of the paper. Another test was conducted under the dry condition, and the contaminants consisted of 0.4 mL of oil, 0.3 g of clay, and 0.4 mL of ethanol. The contaminants and glass beads were mixed together in a tubular shaker, and then paper specimens were put into the shaker and mixed with the contaminants for 30 min. The specimens were then removed and wiped with a wet towel followed by a dry towel. Anti-soiling performance under the dry condition was measured

by ΔE and ISO brightness. The CIELAB color and ISO brightness were measured using an Elrepho spectrophotometer (AB Lorentzen & Wettre, Stockholm, Sweden).

SEM and energy dispersive spectrometer (EDS) analysis

The surface of the paper before and after the soiling test was observed by SEM. The specimens were air dried and sputter coated with platinum. The SEM images of the specimens were obtained by a SUPRA 55-VP. The presence of the PU-CNM coating and dirt on the paper specimen was confirmed by detecting nitrogen, aluminum, and silicon by EDS (XFlash Detector 4010, Bruker, USA) with a working distance of 8.5 mm and an accelerating voltage of 5 kV.

RESULTS AND DISCUSSION

Characteristics of PU-CNM Suspension

The dispersion stability of the PU-CNM suspension was quantitatively evaluated over time. As the first transmission (T) was greater than 0.2%, turbidity was evaluated based on the transmission values. Figure 2 shows the change in the transmission of PU8C2, PU6C4, PU8T2, and PU6T4 suspensions over 12 h. For PU8C2 and PU6C4, there was a very small variation, less than 5%, of the transmission rate over time. Therefore, it was confirmed that the CNC were well dispersed and maintained stability in the PU suspension.

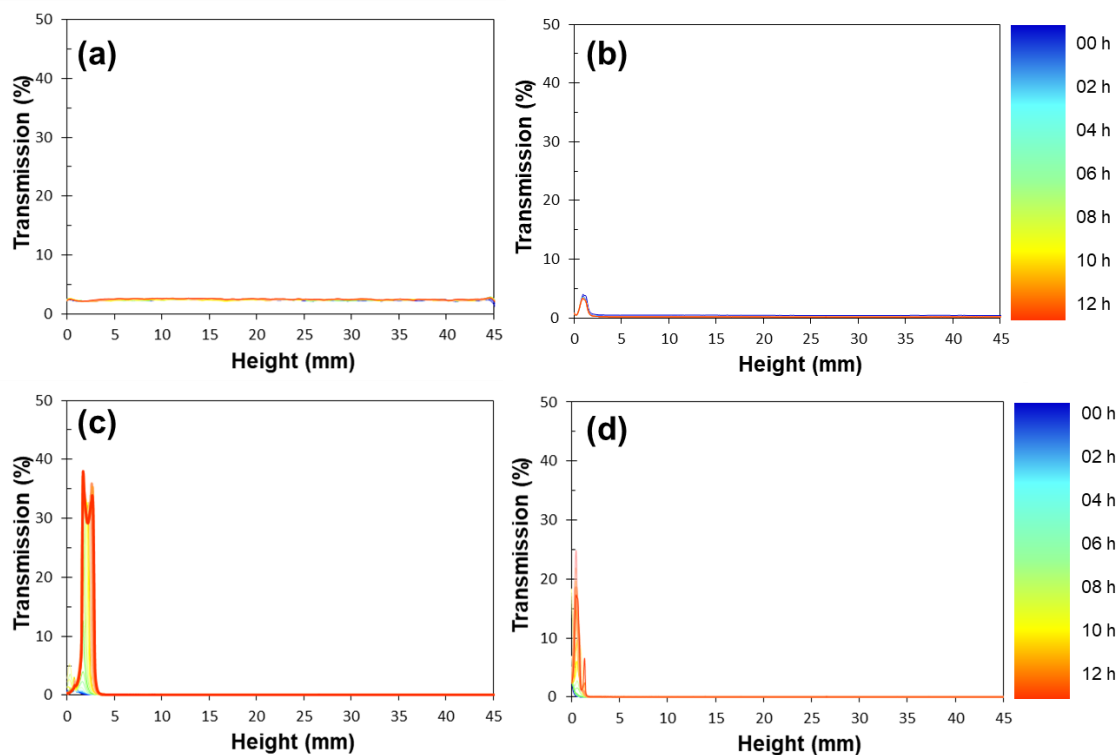


Fig. 2. Profile of T (%) over time: (a) PU8C2 suspension, (b) PU6C4 suspension, (c) PU8T2 suspension, and (d) PU6T4 suspension

In contrast, the transmission rate at the bottom of the PU-TOCN suspension vial quickly changed after 7 h, indicating that phase separation between the TOCN and the

PU occurred. Even though phase separation was observed, it is expected that the PU-TOCN suspension is sufficiently stable to apply as a coating because no aggregation was visible within 7 h.

Figure 3 presents the low-shear viscosity measurements of the suspensions depending on the mixing ratio of CNM. The viscosity of the PU-TOCN increased exponentially with the addition of TOCN, whereas the viscosity of the PU-CNC was not affected by the addition of CNC. This was likely the result of TOCN's much greater viscosity compared to that of the CNC. The viscosity of the CNC (2%) and TOCN (0.95%) were 52 cPs and 1174 cPs, respectively. Despite TOCN's high viscosity, suspensions with the selected mixing ratios had relatively low viscosities, sufficient for application in paper coatings. The PU8T2 and PU6T4 suspensions showed viscosities of 114 cPs and 292 cPs, respectively, which were similar with those of the PU8C2 and PU6C4 suspensions (134 cPs and 152 cPs).

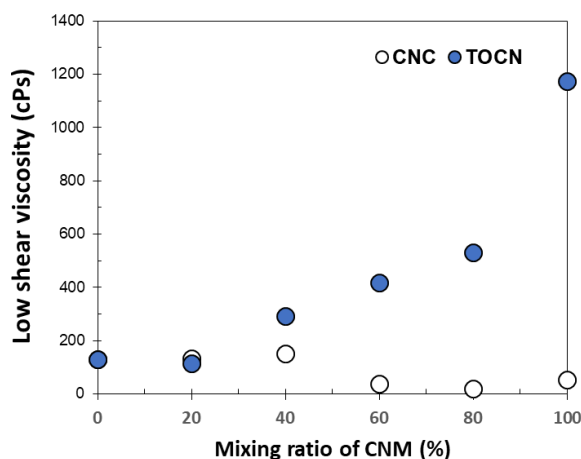


Fig. 3. Low-shear viscosities of the PU-CNM suspensions depending on the mixing ratio of CNM

Mechanical Strength of the Coated Paper

Figure 4 shows the coat weight of the PU-CNM on papers depending on different mixing ratios. The coat weight decreased when increasing the mixing ratio of CNC and TOCN, which resulted from the decrease of the solid content of the suspension.

The mechanical strength of the paper as coated with PU-CNC and PU-TOCN is presented in Fig. 5. The tensile strength of the base paper was enhanced greatly by coating it with all mixing conditions of the PU-CNM suspensions (Fig. 5(a)) because PU coating positively affected on mechanical strength (García-Pacios *et al.* 2011). In particular, paper coated with the PU-TOCN suspensions exhibited the greatest tensile strength even though the dry weight ratio of the TOCN based on PU was less than 2% in both mixing ratios. The tensile strength of the PU-TOCN coated papers was enhanced by increasing the mixing ratio of the TOCN. In contrast, the PU-CNC coated papers showed a slight decrease in the tensile strength with the addition of CNC. There are two reasons for these results. The first reason is based on the characteristics of TOCN, which has a greater aspect ratio than that of CNC (Isogai *et al.* 2011). Therefore, TOCN might have a greater impact on enhancing tensile strength. This can also be confirmed by the fact that the PU6T4-coated paper had greater tensile strength than that of the PU8T2-coated paper. The second reason is likely due to crosslinking between the PU and CNM *via* polyaziridine.

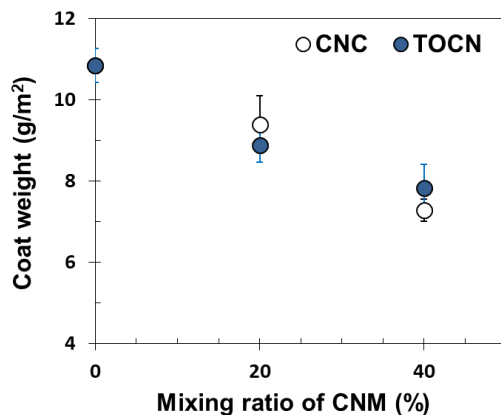


Fig. 4. Coat weight of the coated papers depending on the mixing ratio of the CNM. The error bar represents the standard deviation.

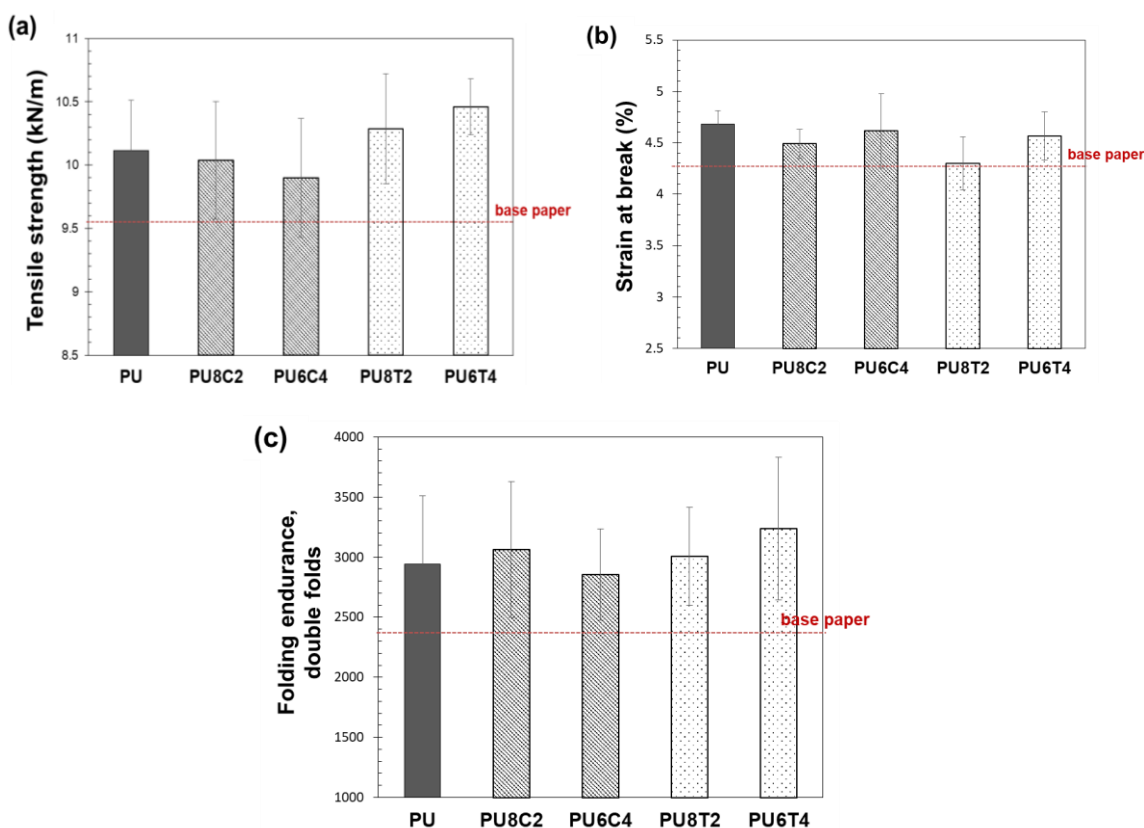


Fig. 5. The (a) tensile strength, (b) strain at break, and (c) folding endurance of the coated paper depending on the mixing conditions of the PU-CNM suspensions. The error bar represents the standard deviation.

Polyaziridine is known for reacting with the carboxyl groups present in PU at ambient temperature to crosslink the PU network (Ollé *et al.* 2008; Xia and Larock 2011), as shown in Fig. 6. The carboxyl groups of PU make aziridine rings open to form ester groups. Therefore, TOCN containing carboxylic acid could be expected to bond with carboxylic acid of PU strongly *via* aziridine. In contrast, CNC would be less crosslinked

with PU because CNC has mainly sulfonate functional groups. Thus, the decrease in tensile strength with increasing mixing ratio of CNC can be explained by weaker crosslinking *via* aziridine as well as decreased coat weight.

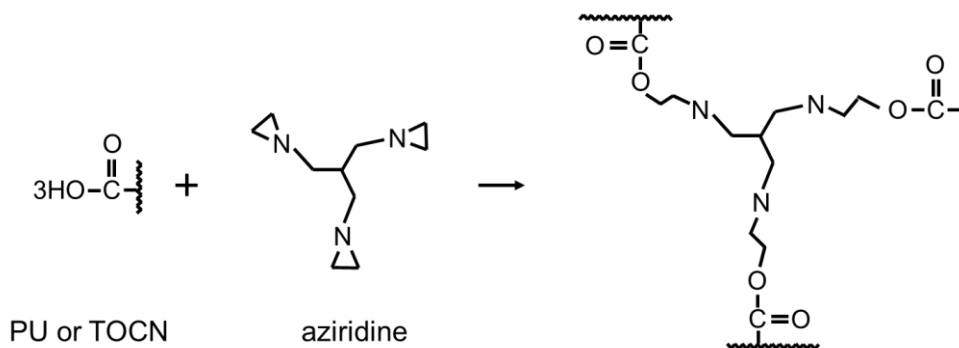


Fig. 6. Crosslinking reaction scheme of PU *via* polyaziridine (Ollé *et al.* 2008)

Both coatings, PU-TOCN and PU-CNC, resulted in a significant improvement in the folding endurance compared with that of the base paper. This is similar to the result obtained in a previous study that reported that PU considerably improved the folding endurance of paper (Guo *et al.* 2014). Folding endurance can be affected by flexibility and crosslinking density of the coating layer (Zhu *et al.* 2016). By the formation of flexible PU-CNM coating layers on the paper, folding endurance could be significantly enhanced. Unlike tensile strength, the PU-CNC coated papers showed a similar level of folding endurance to the PU-TOCN coated papers, despite PU-CNC's weaker bonding force. This result might be caused by PU-CNC showing higher strain than PU-TOCN (Fig. 5(b)), which indicates that folding endurance is the result of the synergistic effect between flexibility and crosslinking between the PU and the CNM.

Anti-soiling Performance of Coated Paper

Anti-soiling tests were performed under wet and dry soiling conditions. For PU-CNC, the wet soiling test was only conducted with a mixing ratio of 80:20, which exhibited better mechanical strength. Figure 7 shows photographs of the contaminated papers after the wet soiling test. The PU-CNM coated papers appeared brighter than the base paper. To evaluate the anti-soiling performance quantitatively, the color difference (ΔE) from before and after the wet soiling test was ascertained (Fig. 8). There was a notable reduction in ΔE for all the coating conditions, including a 50% reduction when compared with the base paper for the 10 min test. The remarkable reduction of ΔE in the PU-CNM coated papers was because the PU used in this study was synthesized by polycarbonate diols. Such PU is known for great mechanical strength and weathering resistance because the polycarbonates are characterized by strong carbonate bonds (García-Pacios *et al.* 2011). The PU-CNC coated paper had a lower ΔE value in the 10 min test than the PU-TOCN coated papers; however, the PU-TOCN coated papers showed lower values in tests longer than 10 min. This means the PU-TOCN coating is better resistance to long-term contamination.

In the dry soiling tests, the ΔE values of the PU8T2 and PU6T4 coated papers were reduced by 27% and 23%, respectively, as compared with the base paper (Fig. 9). They were also lower than that of the PU-CNC coated paper. Furthermore, the PU-TOCN coated papers had greater ISO brightness values than the PU-CNC coated paper after

contamination. This result also confirms that crosslinking between the PU and TOCN might improve soiling resistance. Comparing PU-only coated papers and PU-TOCN coated papers also revealed a greater dry soiling resistance in the PU-TOCN coated papers. Therefore, it can be concluded that adding a small amount of TOCN enhanced the dry soiling resistance performance of the PU coating.

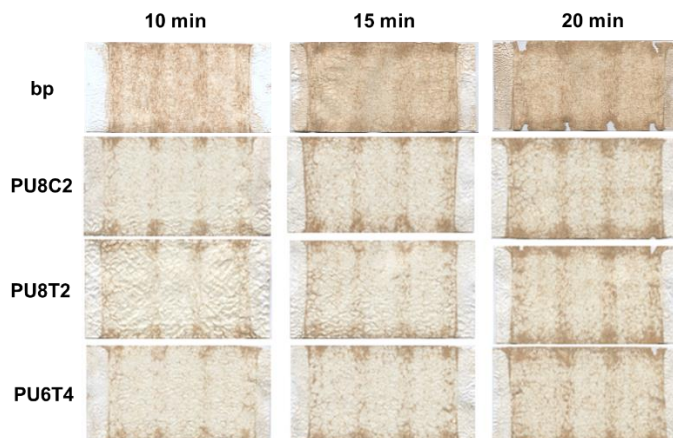


Fig. 7. Photographs of the coated paper after the wet soiling test depending on the PU-CNM mixing conditions and soiling test duration; bp – base paper

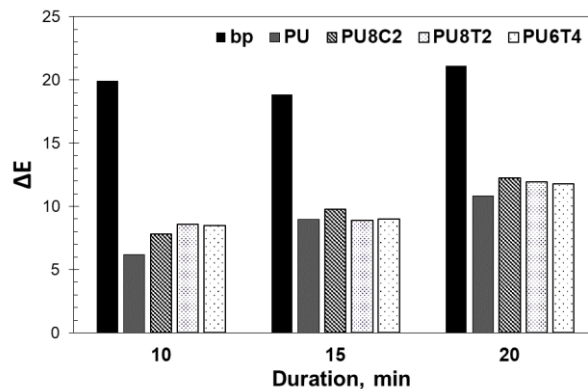


Fig. 8. Color difference (ΔE) depending on the duration of the wet soiling test; bp – base paper

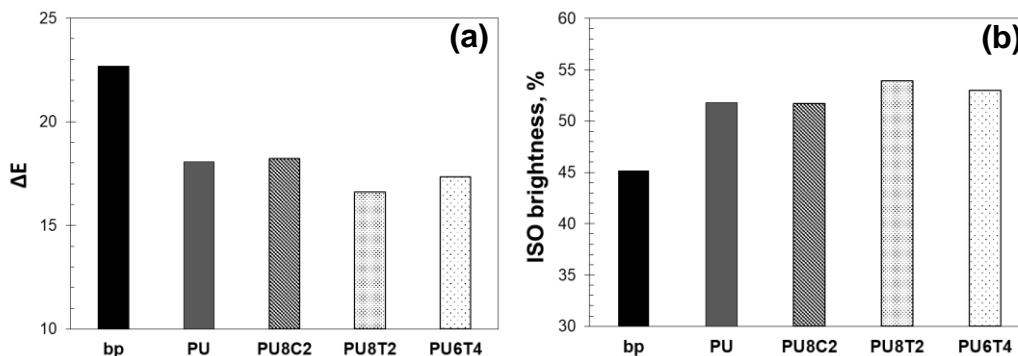


Fig. 9. The (a) color difference (ΔE) and (b) brightness values of the coated papers with different PU-CNM suspensions in the dry soiling test; bp – base paper

SEM and EDS Analysis

Figure 10 shows the SEM images of the paper coated with the PU8C2 suspension before and after the wet soiling test for 15 min. Before the wet soiling test, the PU-CNM coating layer completely covered the surface of the paper to form a smooth surface. However, after the soiling test, the fibers were exposed again because the PU-CNM coating layer peeled off due to physical impact during the soiling test. This behavior was also observed in the PU and PU-TOCN coated papers.

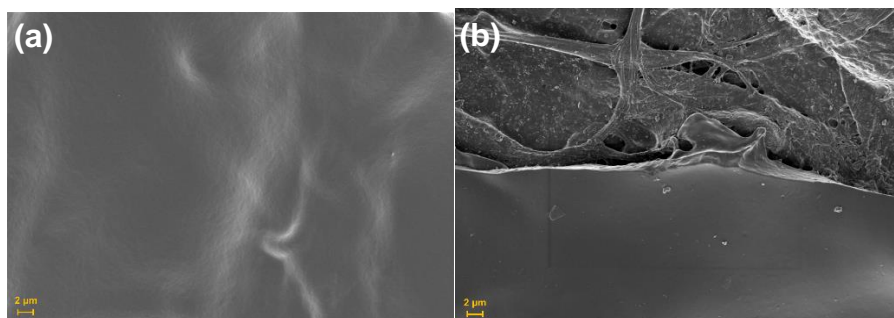


Fig. 10. SEM images of PU8C2-coated paper (a) before and (b) after the wet soiling test

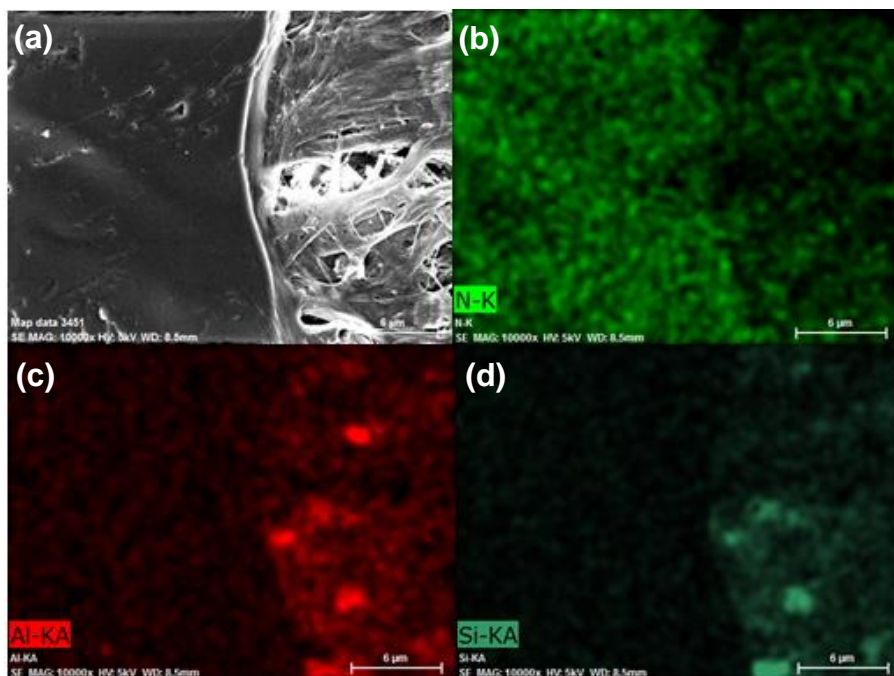


Fig. 11. The (a) SEM image and (b)-(d) EDS mapping analysis of the surface of the PU6T4-coated paper after the wet soiling test: (b) Na-mapping, (c) Al-mapping, and (d) Si-mapping

The EDS analysis of the PU6T4-coated paper after the wet soiling test for 15 min is shown in Fig. 11. The EDS mapping was performed to observe the distribution of contaminants and the PU-CNM coating. A clear boundary can be observed between a part of the coating that peeled off and a part that remained from the centers of the images. The distribution of nitrogen was different around this line; on the right side, less nitrogen was present, showing that the fibers were revealed after the PU-CNM coating peeled off. Furthermore, Figs. 11(c) and 11(d) show the distributions of aluminum and silicon derived

from vermiculite, that were part of the colored powder of the contaminants used in the wet soiling test. They were more concentrated on the exposed fibers found on the right sides of the images. The presence of aluminum and silicon was clearly divided at the boundary, indicating that the PU-CNM coating protected the paper from being worn out and contaminated. Accordingly, the key factor behind the anti-soiling property of the coated paper was the formation and adhesion of the PU-CNM coating layer on the surface. The papers coated with PU-TOCN exhibited stronger bonding between the PU and TOCN, resulting in good adhesion on the surface and the best anti-soiling effect.

CONCLUSIONS

1. When mixing the polyurethane (PU) and cellulose nanomaterial (CNM), the viscosity of PU-TOCN increased with the addition of TEMPO-oxidized cellulose nanomaterial (TOCN), whereas the viscosity of PU-CNC was not affected by the incorporation of cellulose nanocrystals (CNC). Evaluating the miscibility between the PU and CNM, the PU-TOCN suspension was less stable than the PU-CNC suspension. However, no negative effects were found when applying the PU-TOCN suspension in coatings within 7 h.
2. The PU-CNM coated papers exhibited significantly greater mechanical strength and improved soiling resistance in comparison to the base paper. In particular, the PU-TOCN coated papers exhibited greater mechanical strength and soiling resistance than those exhibited by the PU-CNC coated papers. This result was not only because TOCN has a greater aspect ratio than CNC but also because crosslinking *via* polyaziridine between the PU and TOCN was more active than with the CNC, resulting in stronger inter-bonding.
3. The scanning electron micrograph (SEM) images and energy dispersive spectrometer (EDS) mapping analysis confirmed that fibers were exposed after the PU-CNM coating layer was removed in the soiling tests. Aluminum and silicon, which were components of contaminants, were adsorbed onto the exposed fibers. Therefore, the formation and adhesion of the PU-CNM coating layer was critical in fabricating durable, anti-soiling paper.

ACKNOWLEDGMENTS

This work was supported by the Technology Innovation Program (No. 10067241, Development of application technology of nanocellulose for manufacture of specialty paper with high security and durability) and was funded by the Ministry of Trade, Industry & Energy (MOTIE, Korea). The authors express their appreciation to T&L Co., Stahl, Hansol, and KOMSCO for providing the materials used in this study.

REFERENCES CITED

- Abdul Khalil, H. P. S., Bhat, A. H., and Yusra, A. F. I. (2012). "Green composites from sustainable cellulose nanofibrils: A review," *Carbohydrate Polymers* 87(2), 963-979. DOI: 10.1016/j.carbpol.2011.08.078
- Akindoyo, J. O., Beg, M. D. H., Ghazali, S., Islam, M. R., Jeyaratnam, N., and Yuvaraj, A. R. (2016). "Polyurethane types, synthesis and applications – A review," *RSC Advances* 6(115), 114453-114482. DOI: 10.1039/C6RA14525F
- Çanak, T. Ç., and Serhatlı, İ. E. (2013). "Synthesis of fluorinated urethane acrylate based UV-curable coatings," *Progress in Organic Coatings* 76(2-3), 388-399. DOI: 10.1016/j.porgcoat.2012.10.024
- Cataldi, P., Ceseracciu, L., Marras, S., Athanassiou, A., and Bayer, I. S. (2017). "Electrical conductivity enhancement in thermoplastic polyurethane-graphene nanoplatelet composites by stretch-release cycles," *Applied Physics Letters* 110(12), 121904. DOI: 10.1063/1.4978865
- Cataldi, P., Profaizer, M., and Bayer, I. S. (2019). "Preventing water-induced mechanical deterioration of cardboard by a sequential polymer treatment," *Industrial & Engineering Chemistry Research* 58(16), 6456-6465. DOI: 10.1021/acs.iecr.9b00712
- Chattopadhyay, D. K., and Raju, K. V. S. N. (2007). "Structural engineering of polyurethane coatings for high performance applications," *Progress in Polymer Science* 32(3), 352-418. DOI: 10.1016/j.progpolymsci.2006.05.003
- Cheng, D., Wen, Y., An, X., Zhu, X., and Ni, Y. (2016). "TEMPO-oxidized cellulose nanofibers (TOCNs) as a green reinforcement for waterborne polyurethane coating (WPU) on wood," *Carbohydrate Polymers* 151, 326-334. DOI: 10.1016/j.carbpol.2016.05.083
- Chuang, F. S., Tsi, H. Y., Chow, J. D., Tsen, W. C., Shu, Y. C., and Jang, S. C. (2008). "Thermal degradation of poly (siloxane-urethane) copolymers," *Polymer Degradation and Stability* 93(10), 1753-1761. DOI: 10.1016/j.polymdegradstab.2008.07.029
- Fan, W., Du, W., Li, Z., Dan, N., and Huang, J. (2015). "Abrasion resistance of waterborne polyurethane films incorporated with PU/silica hybrids," *Progress in Organic Coatings* 86, 125-133. DOI: 10.1016/j.porgcoat.2015.04.022
- Fan, W., Zhu, Y., Xi, G., Huang, M., and Liu, X. D. (2016). "Wear-resistant cotton fabrics modified by PU coatings prepared *via* mist polymerization," *Journal of Applied Polymer Science* 133(7). DOI: 10.1002/app.43024
- Florian, P., Jena, K. K., Allauddin, S., Narayan, R., and Raju, K. V. S. N. (2010). "Preparation and characterization of waterborne hyperbranched polyurethane-urea and their hybrid coatings," *Industrial & Engineering Chemistry Research* 49(10), 4517-4527. DOI: 10.1021/ie900840g
- Gao, Z., Peng, J., Zhong, T., Sun, J., Wang, X., and Yue, C. (2012). "Biocompatible elastomer of waterborne polyurethane based on castor oil and polyethylene glycol with cellulose nanocrystals," *Carbohydrate Polymers* 87(3), 2068-2075. DOI: 10.1016/j.carbpol.2011.10.027
- García-Pacios, V., Iwata, Y., Colera, M., and Martín-Martínez, J. M. (2011). "Influence of the solids content on the properties of waterborne polyurethane dispersions obtained with polycarbonate of hexanediol," *International Journal of Adhesion and Adhesives* 31(8), 787-794. DOI: 10.1016/j.ijadhadh.2011.05.010
- Guo, Y. H., Guo, J. J., Miao, H., Teng, L. J., and Huang, Z. (2014). "Properties and paper

- sizing application of waterborne polyurethane emulsions synthesized with isophorone diisocyanate,” *Progress in Organic Coatings* 77(5), 988-996. DOI: 10.1016/j.porgcoat.2014.02.003
- Hung, K. C., Tseng, C. S., and Hsu, S. H. (2014). “Synthesis and 3D printing of biodegradable polyurethane elastomer by a water-based process for cartilage tissue engineering applications,” *Advanced Healthcare Materials* 3(10), 1578-1587. DOI: 10.1002/adhm.201400018
- ISO 1924-2 (2008). “Paper and board – Determination of tensile properties – Part 2: Constant rate of elongation method (20 mm/min),” International Organization for Standardization, Geneva, Switzerland.
- ISO 5626 (1993). “Paper – Determination of folding endurance,” International Organization for Standardization, Geneva, Switzerland.
- Isogai, A., Satio, T., and Fukuzumi, H. (2011). “TEMPO-oxidized cellulose nanofibers” *Nanoscale* 3(1), 71-85. DOI: 10.1039/C0NR00583E
- Lei, W., Zhou, X., Fang, C., Song, Y., and Li, Y. (2019). “Eco-friendly waterborne polyurethane reinforced with cellulose nanocrystal from office waste paper by two different methods,” *Carbohydrate Polymers* 209, 299-309. DOI: 10.1016/j.carbpol.2019.01.013
- Mazzon, G., Zahid, M., Heredia-Guerrero, J. A., Balliana, E., Zendri, E., Athanassiou, A., and Bayer, I. S. (2019). “Hydrophobic treatment of woven cotton fabrics with polyurethane modified aminosilicone emulsions,” *Applied Surface Science* 490, 331-342. DOI: 10.1016/j.apsusc.2019.06.069
- Meng, Q. B., Lee, S. I., Nah, C., and Lee, Y. S. (2009). “Preparation of waterborne polyurethanes using an amphiphilic diol for breathable waterproof textile coatings,” *Progress in Organic Coatings* 66(4), 382-386. DOI: 10.1016/j.porgcoat.2009.08.016
- Mishra, A. K., Narayan, R., Raju, K. V. S. N., and Aminabhavi, T. M. (2012). “Hyperbranched polyurethane (HBPU)-urea and HBPU-imide coatings: Effect of chain extender and NCO/OH ratio on their properties,” *Progress in Organic Coatings* 74(1), 134-141. DOI: 10.1016/j.porgcoat.2011.11.027
- Noble, K. L. (1997). “Waterborne polyurethanes” *Progress in Organic Coatings* 32(1-4), 131-136. DOI: 10.1016/S0300-9440(97)00071-4
- Noreen, A., Zia, K. M., Zuber, M., Tabasum, S., and Saif, M. J. (2016). “Recent trends in environmentally friendly water-borne polyurethane coatings: A review,” *Korean Journal of Chemical Engineering* 33(2), 388-400. DOI: 10.1007/s11814-015-0241-5
- Ollé, L., Bacardit, A., Morera, J. M., Bartolí, E., and Argelich, J. (2008). “Binders cross-linked with polyaziridine. Study of cross-linked polymers for aqueous finishing. Part I: Behaviour of polyurethane,” *Journal of the Society of Leather Technologists and Chemists* 92(3), 96-102.
- Osman, M. A., Mittal, V., Morbidelli, M., and Suter, U. W. (2003). “Polyurethane adhesive nanocomposites as gas permeation barrier,” *Macromolecules* 36(26), 9851-9858. DOI: 10.1021/ma035077x
- Petrović, Z. S., Zhang, W., Zlatanić, A., Lava, C. C., and Ilavský, M. (2002). “Effect of OH/NCO molar ratio on properties of soy-based polyurethane networks,” *Journal of Polymers and the Environment* 10(1-2), 5-12. DOI: 10.1023/A:1021009821007
- Rahimi, A., and Mashak, A. (2013). “Review on rubbers in medicine: natural, silicone and polyurethane rubbers,” *Plastics, Rubber and Composites* 42(6), 223-230. DOI: 10.1179/1743289811Y.0000000063
- Rahman, M. M., Kim, H. D., and Lee, W. K. (2008). “Preparation and characterization of

- waterborne polyurethane/clay nanocomposite: effect on water vapor permeability,” *Journal of Applied Polymer Science* 110(6), 3697-3705. DOI: 10.1002/app.28985
- Rashvand, M., and Ranjbar, Z. (2013). “Effect of nano-ZnO particles on the corrosion resistance of polyurethane-based waterborne coatings immersed in sodium chloride solution via EIS technique,” *Progress in Organic Coatings* 76(10), 1413-1417. DOI: 10.1016/j.porgcoat.2013.04.013
- Rueda, L., Saralegui, A., Fernández d’Arlas, B., Zhou, Q., Berglund, L. A., Corcuera, M. A., Mondragon, I., and Eceiza, A. (2013). “Cellulose nanocrystals/polyurethane nanocomposites. Study from the viewpoint of microphase separated structure,” *Carbohydrate Polymers* 92(1), 751-757. DOI: 10.1016/j.carbpol.2012.09.093
- Saha, S., Kocaefe, D., Krause, C., and Larouche, T. (2011). “Effect of titania and zinc oxide particles on acrylic polyurethane coating performance,” *Progress in Organic Coatings* 70(4), 170-177. DOI: 10.1016/j.porgcoat.2010.09.021
- Wang, X., Hu, J., Li, Y., Zhang, J., and Ding, Y. (2015). “The surface properties and corrosion resistance of fluorinated polyurethane coatings,” *Journal of Fluorine Chemistry* 176, 14-19. DOI: 10.1016/j.jfluchem.2015.04.002
- Xia, Y., and Larock, R. C. (2011). “Castor-oil-based waterborne polyurethane dispersions cured with an aziridine-based crosslinker,” *Macromolecular Materials and Engineering* 296(8), 703-709. DOI: 10.1002/mame.201000431
- Zhang, H., She, Y., Song, S., Chen, H., and Pu, J. (2012). “Improvements of mechanical properties and specular gloss of polyurethane by modified nanocrystalline cellulose,” *BioResources* 7(4), 5190-5199. DOI: 10.15376/biores.7.4.5190-5199
- Zhou, X., Li, Y., Fang, C., Li, S., Cheng, Y., Lei, W., and Meng, X. (2015). “Recent advances in synthesis of waterborne polyurethane and their application in water-based ink: A review,” *Journal of Materials Science & Technology* 31(7), 708-722. DOI: 10.1016/j.jmst.2015.03.002
- Zhu, K., Li, X., Wang, H., Fei, G., and Li, J. (2016). “Properties and paper sizing application of waterborne polyurethanemicroemulsions: Effects of extender, cross-linker, and polyol,” *Journal of Applied Polymer Science* 133(25). DOI: 10.1002/app.43211

Article submitted: July 18, 2019; Peer review completed: September 3, 2019; Revised version received and accepted: September 23, 2019; Published: September 25, 2019. DOI: 10.15376/biores.14.4.8973-8986